 DOI: 10.1002/masy.201000059

Ethylene Polymerization by Metallocene Catalysts Supported over Siliceous Materials with Bimodal Pore Size Distribution

Jovita Moreno,[*1] *Rafael van Grieken,*[1] *Alicia Carrero,*[2] *Beatriz Paredes*[1]

Summary: As known, the pore structure of the catalytic support plays a decisive role during the polymerization reactions determining intra-particle mass and heat transport phenomena. In this work, several ethylene polymerizations have been carried out by using as catalytic support different mesostructured materials with unimodal and bimodal pore size distributions in order to evaluate the influence of this pore size distribution on the catalytic behavior. Calcined mesoporous materials were impregnated with the catalytic system MAO/$(nBuCp)_2ZrCl_2$ and used for ethylene polymerization and ethylene/1-hexene copolymerizations, at 70 °C and 5 bar of ethylene pressure. Polyethylenes obtained were characterized by GPC, DSC and Crystaf. Results indicate that porous structure of the support has a significant influence on polymerization activity and polymer properties. Despite the catalyst bimodal pore size distribution, only ethylene/1-hexene copolymers presented a bimodal chemical composition distribution.

Keywords: chemical composition distribution; ethylene polymerization; metallocene; pore size distribution

Introduction

Nowadays, continuous advances on polymerization technology and catalysts development allow the production of polyethylene with novel properties.[1-3] In this sense, bimodal polyethylene consisting in two fractions with different molecular weight and comonomer content, has a growing industrial interest since combines good mechanical properties and processability.[4] The traditional process for the production of bimodal resins is a cascade process, using conventional Ziegler-Natta type catalyst.[1] An alternative for the production of bimodal polyethylene avoiding the use of two reactors and reducing the operation costs is based on the induction of polymer bimodality from the catalytic system. With this purpose, several authors have reported the development of multicomponent catalysts by using different catalytic sites with distinctive responses. Results have showed that with these catalysts a blend of polymeric chains with different predominant molecular masses can be obtained in only one-step polymerization process.[5-7]

On the other hand, for heterogeneous catalysts there is the chance to induce the polymer bimodality from the inorganic carrier used as catalytic support. As known, during the polymerization of ethylene by using heterogeneous metallocene catalysts, not only active centres play an important role on the catalytic behaviour but physicochemical properties of the support have also a significant influence.[8] In this context, the use of mesoporous materials with well differentiated systems of pores could generate active sites located in different environments leading to different catalytic

[1] Department of Chemical and Environmental Technology, ESCET, Universidad Rey Juan Carlos, 28933 Mostoles, Spain
E-mail: jovita.moreno@urjc.es
[2] Department of Chemical and Energy Technology, ESCET, Universidad Rey Juan Carlos, 28933 Mostoles, Spain

response and, thus, a possible bimodality in the molecular weight distribution (MWD) and/or in the chemical composition distribution (CCD). This last distribution is also very important for the case of copolymers in order to get a more complete understanding of the active site types and polymer properties.

Some authors have reported the synthesis of mesostructured silicas with a bimodal pore size distribution based on the use of two surfactant micelles with sizes clearly differentiated in the first step of the synthesis.[9] Then, after silica incorporation and material calcination two ordered mesophases can be obtained. Other possibility is a two-step chemical templating route based on the preparation of MCM-41 in the first step (mean pore size around 2.5 nm) which is used as a silica source is the second step, where the larger pores are generated by using Pluronic P-123 as surfactant.[10]

In this work, several unimodal and bimodal pore size distribution supports were prepared by direct synthesis and by physical mixing of different unimodal supports. After impregnation with MAO/$(n\text{BuCp})_2ZrCl_2$ catalytic system, they were tested in ethylene polymerization and ethylene/1-hexene copolymerization. Polyethylene homo and copolymers were characterized to analyze the influence of catalyst pore size distribution on the polymers molecular weight and chemical composition distribution.

Experimental Part

Preparation of Unimodal Mesoporous Materials and Physical Mixtures

SBA-15-type materials were synthesized according to the procedure described by Zhao et al.[11] In a typical synthesis: 4 g of Pluronic 123 triblock copolymer (EO_{20}-PO_{70}-EO_{20}; Aldrich) were dissolved under stirring in 125 g of 1.9 M HCl at room temperature. The solution was heated up to 40 °C before adding 8.6 g of tetraethylorthosilicate (TEOS; Aldrich). The resultant solution was stirred for 20 h at 40 °C, followed by aging for 24 h under static conditions. Two different temperature values (110 and 60 °C) were used for the aging step in order to prepare two SBA-15 materials with different textural properties. After that, the solids were recovered by filtration and dried at room temperature overnight. The template was removed by calcination at 550 °C for 5 h (heating rate = 1.8 °C min^{-1}). Calcined supports were denoted as SBA-15 and SBA-15(60 °C) accordingly to aging temperature (110 °C and 60 °C, respectively).

MCM-41 support was synthesized according to the hydrothermal procedure described by Lin et al. [12] using cetyltrimethylammonium bromide (CTAB; Aldrich) as template and dimethylamine (DMA; 40 wt % in water; Aldrich) as alkaline agent. In a typical synthesis: 2.4 g of CTAB were dissolved under stirring in a mixture of 90.3 g of water and 7.4 g of DMA at room temperature. Then, silica source (TEOS; Aldrich) was added by dropping. The resultant solution was stirred for 4 h and aged at 110 °C during 48 h. The solid was recovered by filtration and dried at room temperature overnight. The template was removed by calcination at 550 °C for 5 h (heating rate = 1.8 °C min^{-1}). This calcined support was denoted as MCM-41.

Two physical mixtures were prepared by using these three mesoporous materials: SBA-15 + SBA-15(60°) and SBA-15 + MCM-41 with a mass ratio of 1:1 in both cases.

Preparation of Bimodal Mesoporous Materials

The material called bimodal-1 was prepared by the same procedure than the SBA-15 support but using as template a mixture of two non-ionic surfactants: Pluronic 123 triblock copolymer (EO_{20}-PO_{70}-EO_{20}; Aldrich) and other triblock copolymer (EO_5-PO_{41}-EO_5; Aldrich). Thus, the 4 g of P123 used in the preparation of SBA-15 material were replaced by a mixture of 2 g of P123 and 2 g of the other template.

The support bimodal-2 was prepared by combination of SBA-15 and MCM-41

synthesis procedures. Thus, 4 g of Pluronic 123 were dissolved under stirring in 125 g of 1.9 M HCl at room temperature. The solution was heated up to 40 °C and then 8.6 g of TEOS were added leading to the solution A. On the other hand, 2.4 g of CTAB were dissolved under stirring in a mixture of 90.3 g of water and 7.4 g of DMA at room temperature. Then, TEOS was added by dropping leading to the B solution. Both solutions were maintained under stirring at 40 °C during 20 h before mixing, and the resulting gel was aged at 110 °C for 36 h. Templates were removed by calcination at 550 °C for 5 h (heating rate = 1.8 °C min^{-1}).

Characterization of Mesoporous Materials

Nitrogen adsorption-desorption isotherms at 77 K of supports and catalysts were obtained with a Micromeritics Tristar 3000 apparatus. Surface areas were calculated with BET equation whereas pore size distributions were determined by the BJH method applied to the adsorption branch of the isotherms. Mean pore size was obtained from the maximum of BJH pore size distribution. X-ray powder diffraction (XRD) data were acquired on a Philips X'PERT MPD diffractometer using Cu Kα radiation. Low angle XRD patterns ($0.6° < 2\theta < 5°$) were obtained using a step size of 0.02° and a counting time of 5 s. Transmission electron micrographs (TEM) were collected on a Phillips TECNAI 20 microscope equipped with a LaB_6 filament under an accelerating voltage of 200 kV.

Preparation of Supported Metallocene Catalysts and Polymerization Reactions

The metallocene bis(n-butylcyclopentadienyl)zirconium dichloride ($(nBuCp)_2ZrCl_2$, 97%, Aldrich), was dissolved at room temperature in a solution of methylaluminoxane (MAO, 10 wt% in toluene, Aldrich) previously diluted with dry toluene (99 wt%, Scharlab), having a molar ratio Al_{MAO}/Zr of 190. Then, the contact between the carrier and the described solution was carried out at room temperature, in a stirred vessel during 3 hours. Finally, the solid was dried under nitrogen flow and stored in glove-box. Aluminium and zirconium contents of the supported catalysts were determined by ICP-AES on a Varian Vista AX Axial CCD Simultaneous ICP-AES spectrophotometer.

Ethylene polymerizations were performed at 70 °C in a 1.0-L stirred-glass reactor filled with 600 cm^3 of n-heptane (99%, Scharlab) as diluent, and tri-isobutylamunimum (TIBA, 30 wt% in heptane, Witco) as scavenger. The monomer (Ethylene, 99.99%, Air Liquide) was fed to the reactor as it was demanded to keep a total pressure of 5 bar. After 30 minutes, the polymerization was stopped by depressurization and polyethylene (PE) was recovered, filtered and dried for 12 hours at 70 °C. For ethylene/1-hexene copolymerizations, 50 mL of 1-hexene were added to the reactor.

Polymer Characterization

Molecular weights and polydispersity indexes were determined with a Waters ALLIANCE GPCV 2000 gel permeation chromatograph (GPC) equipped with a refractometer, a viscosimeter and three Styragel HT type columns (HT3, HT4 and HT6) with exclusion limit 1×10^7 for polystyrene. 1,2,4-Trichlorobenzene was used as solvent, at a flow rate of 1 cm^3 min^{-1}. The analyses were performed at 145 °C. The columns were calibrated with standard narrow molar mass distribution polystyrenes and with linear low density polyethylenes and polypropylenes. Polymer melting points (T_m), crystallization temperatures (T_c) and crystallinities were determined in a METTLER TOLEDO DSC822 differential scanning calorimeter (DSC), using a heating rate of 10 °C min^{-1} in the temperature range 23–160 °C. The heating cycle was performed twice, but only the results of the second scan are reported, because the former is influenced by the mechanical and thermal history of the samples. Chemical composition distributions were measured by Crystaf (Polymer Char) using 1,2,4-trichlorobenzene as a solvent. Dissolution took place at 160 °C

for 90 min followed by equilibration at 95 °C for 45 min. The crystallization rates were 0.1 °C/min from 95 to 19 °C. A two channel infrared detector was used to measure the concentration of polymer in the solution during crystallization. A BRUKER AC300 spectrometer at 75 MHz was used to characterize the copolymers by ^{13}C NMR measurement and determine their 1-hexene molar fraction. The samples were added into sample tube with the mixture of 1,2,4-trichlorobenzene and 1,1,2,2-tetrachloroethylane-d_2 in a concentration of 10 vol%.

Results and Discussion

Figure 1 presents the nitrogen adsorption-desorption isotherms at 77 K and the BJH pore size distribution of the individual materials and the corresponding physical mixtures. All the solids show type IV adsorption isotherm in the IUPAC classification, a typical shape for mesoporous MCM-41 and SBA-15 materials.[11,12] Three well-distinguished regions of the adsorption isotherm are evident: (i) monolayer-multilayer adsorption, (ii) capillary condensation, and (iii) multilayer adsorption on the outer particle surfaces. Apart from MCM-41 material, a clear type-H1 hysteresis loop is observed, and the capillary condensation occurs at a higher relative pressure for SBA-15 materials, which is related to the bigger pore size[12] The isotherms of the physical mixtures show the features of the individual materials isotherms, and as it can be observed in the pore size distributions, where there is a contribution of each material according to the 50/50 wt% mixture prepared. However,

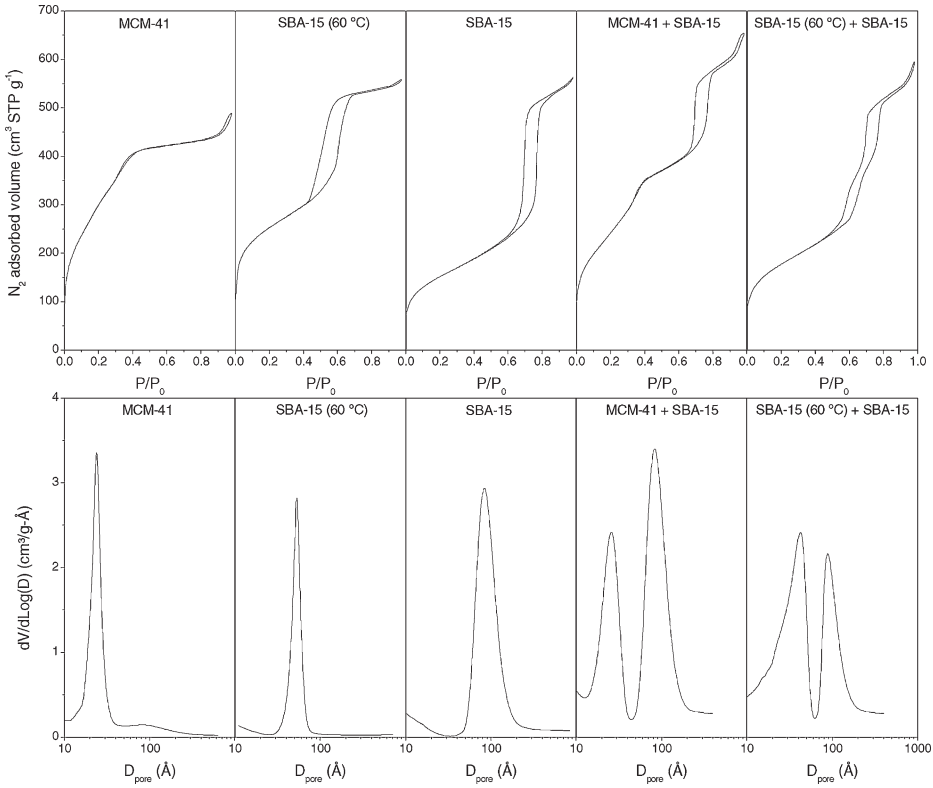

Figure 1.
N_2 adsorption-desorption isotherms at 77 K and BJH pore size distribution of the individual materials and the corresponding physical mixtures.

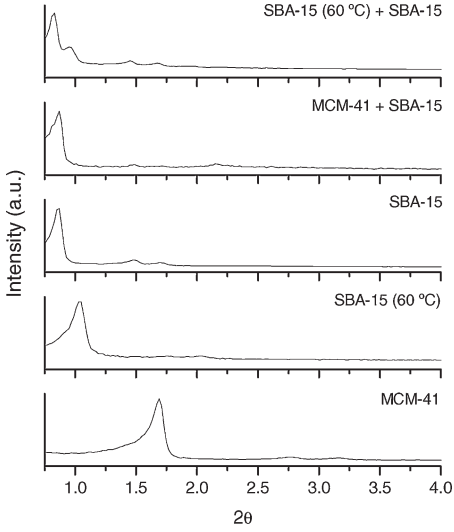

Figure 2.
X-ray diffraction patterns of the individual materials and the corresponding physical mixtures.

it is a little bit difficult to distinguish that contribution by XRD (Figure 2) for MCM-41 + SBA-15 physical mixture, not for SBA-15's mixture in which it is possible to observe a peak and a shoulder corresponding to both different unit cells from the individual materials. The reflections come from the ordered hexagonal array of parallel silica tubes and they can be indexed assuming a hexagonal unit cell; since the materials are not crystalline at the atomic level, no reflections at higher angles are observed. The mentioned ordered hexagonal array (honeycomb structure) can be easily observed by transmission electron microscopy (Figure 3).

Mesoporous materials synthesized by mixing surfactants gave bimodal pore size distributions, as can be observed in Figure 4. However, the contribution of each pore size is quite different for both materials, mainly in Bimodal-2 material, for which the same diffraction pattern as SBA-15 material has been determined (Figure 5). Bimodal-1 presents lack of well-defined XRD reflexions suggesting a poor arrangement and instability of the synthesized material, although is possible to observe some ordered regions by TEM in contrast with Bimodal-2 (Figure 6).

All the described materials were employed as supports of the catalytic system MAO/$(n\text{BuCp})_2ZrCl_2$. Table 1 summarizes the physical properties of the supports as well as the aluminium and zirconium contents of the supported catalysts determined by ICP-AES.

Figure 7 shows the polymerization activity of the prepared catalysts in ethyl-

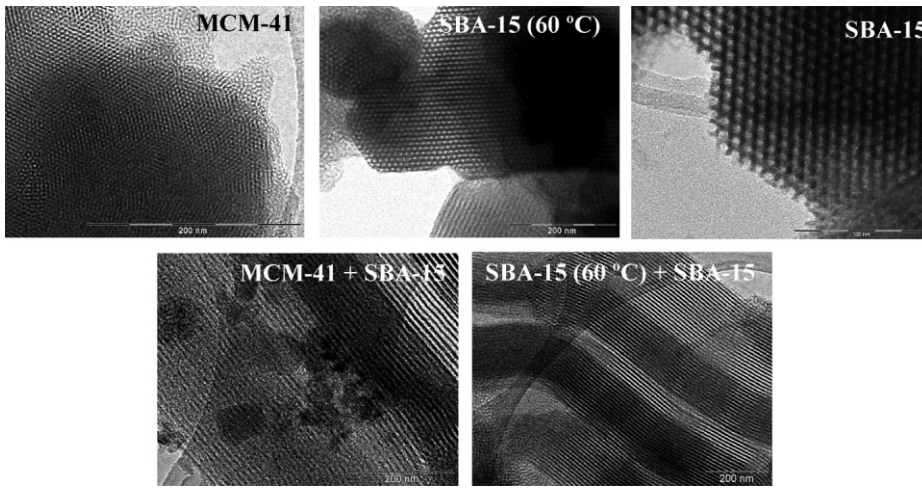

Figure 3.
Transmission electron micrographs of the individual materials and the corresponding physical mixtures.

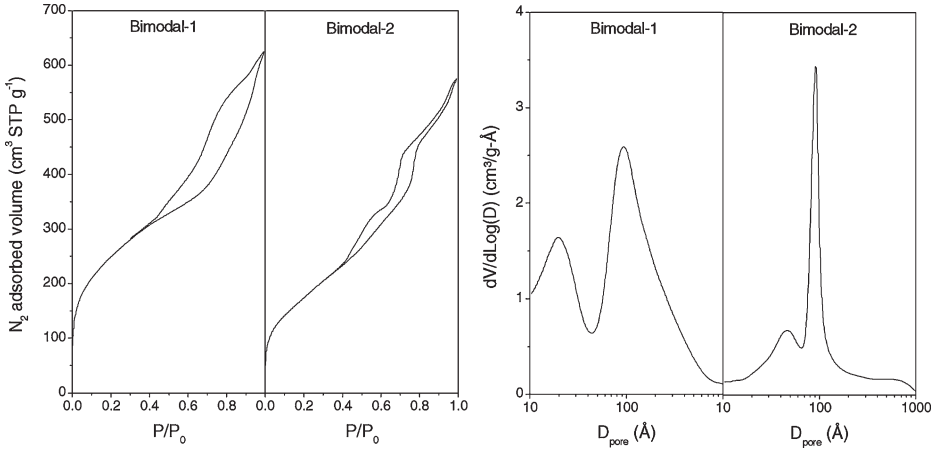

Figure 4.
N_2 adsorption-desorption isotherms at 77 K and BJH pore size distribution of the supports synthesized by mixing surfactants.

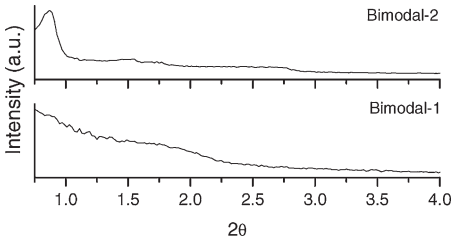

Figure 5.
X-ray diffraction patterns of the supports synthesized by mixing surfactants.

ene homopolymerization and ethylene-1-hexene copolymerization.

In general, catalysts with larger pores presented higher activity in ethylene polymerization; even for samples having also smaller pores like is the case of catalysts prepared with bimodal pore size distribution supports. Such results could suggest that the lower activity can be related to limited MAO/metallocene presence in smaller pores or monomer diffusion limitations to the metallic centres within channels of small diameter, which is in accordance with results showed by F. Silveira et al.,[13] who also studied $(n\text{BuCp})_2ZrCl_2$ catalytic system. However, Kumkaew et al.[14,15] found maximum activities for the afore mentioned catalytic system in gas-phase ethylene polymerization with catalysts prepared with supports having pore diameters in the 2–6 nm range. They explained this behaviour based on the works of Sano

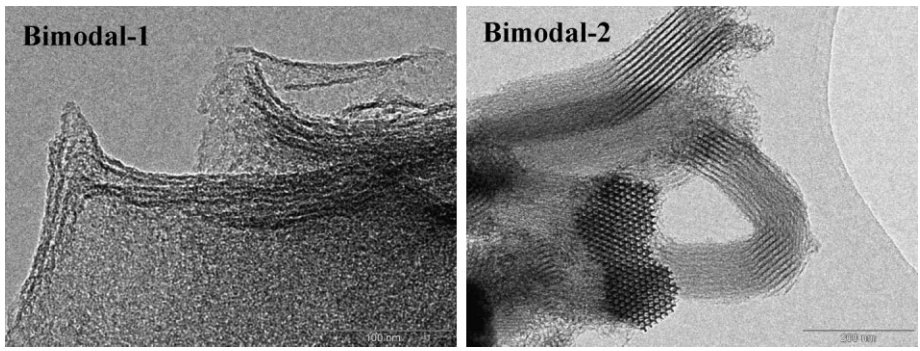

Figure 6.
Transmission electron micrographs of the supports synthesized by mixing surfactants.

Table 1.
Physical properties of the supports and aluminium and zirconium loadings in the supported catalysts.

Porous distribution	Support	A_{BET} (m^2g^{-1})	V_{pore} (cm^3g^{-1})	D_{pore} (nm) [a]	Al (wt%)	Zr (wt%)
Unimodal	MCM-41	994	0.69	2.3	13.5	0.24
	SBA-15 (60 °C)	447	0.43	5.3	14.2	0.25
	SBA-15	822	1.29	8.2	13.1	0.24
Bimodal by physical mixture	MCM-41 + SBA-15	884	0.99	2.5 – 8.1	13.6	0.24
	SBA-15 (60 °C) + SBA-15	638	0.89	4.5 – 8.4	13.9	0.24
Bimodal by direct synthesis	Bimodal-1	602	0.61	2.0 – 9.3	12.9	0.23
	Bimodal-2	644	0.86	4.6 – 9.1	12.8	0.22

[a]Determined from the maximum of BJH pore size distribution.

et al.[16–18] having into account that the most active MAO species responsible for activating metallocenes are preferentially adsorbed by the mesoporous molecular sieves with smaller pores or possibly even stabilized by interaction with the surfaces of the smaller pores. In a previous work employing SBA-15 type materials as carrier[19] we also observed a decrease in polymerization activity by increasing the pore size of the support in the 8.8–22.7 nm range, so there must be an optimum pore size for SBA-15 materials and MAO/$(n\text{BuCp})_2ZrCl_2$ system in slurry ethylene polymerization around 9 nm; therefore, the pore size should be small enough for MAO stabilization but big enough for the anchorage of the catalytic system and not to hinder monomer diffusion.

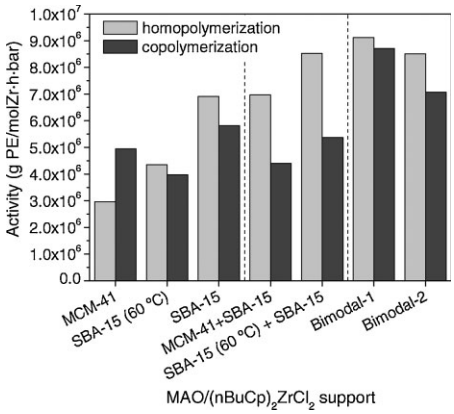

Figure 7.
Polymerization catalytic activity of MAO/$(n\text{BuCp})_2ZrCl_2$ supported over different siliceous materials.

On the other hand, in copolymerization is difficult to establish a trend with catalytic support pore size, because the comonomer effect may be different from one to another supported catalyst. Several works[20–24] that analyze the comonomer effect on the catalytic activity at different comonomer concentrations with supported metallocene catalysts showed a maximum value of activity for a given 1-hexene concentration. That is, at lower comonomer concentrations an activity enhancement is observed, may be related with easier monomer diffusion,[25] while at higher comonomer concentrations an increase of the comonomer fraction in the polymeric growing chain leads to a reduction in activity because of a decrease in the propagation rate.[21,26] It is also possible that the copolymer made at such high comonomer concentration could be too "soft" to break the support particles effectively, causing the reduction of the apparent catalytic activity because some active sites do not show up. So, the support pore size can influence the 1-hexene concentration at which the catalytic activity reaches its maximum. It is remarkable that bimodal supports prepared by direct synthesis present the higher copolymerization activity values. These results are in agreement with those reported by Bunchongturakarn et al.[27] who also found a higher catalytic activity for ethylene/1-octene copolymerization of a zirconocene catalytic system supported in a bimodal MCM-41 compared to the unimodal one.

Finally, it must be also mentioned that, apart from MCM-41 catalyst, all the supported catalysts show a lower copoly-

Table 2.
Characterization of ethylene homopolymers.

Porous distribution	Support	M_w (g/mol)	M_w/M_n	T_m (°C)	α (%)
Unimodal	MCM-41	218967	2.14	137.4	59.2
	SBA-15 (60 °C)	173668	2.20	135.1	62.2
	SBA-15	167292	2.10	133.4	63.2
Bimodal by physical mixture	MCM-41 + SBA-15	221751	2.20	137.4	62
	SBA-15 (60 °C) + SBA-15	199791	2.15	135.5	60.7
Bimodal by direct synthesis	Bimodal-1	208004	2.14	136	61.8
	Bimodal-2	215860	2.12	137	62.5

Table 3.
Characterization of ethylene-1-hexene copolymers.

Porous distribution	Support	M_w (g/mol)	M_w/M_n	T_m (°C)	α (%)	1-hex (mol%)
Unimodal	MCM-41	242769	2.22	104.3	24.3	2.91
	SBA-15 (60 °C)	169122	2.98	105.6	27.8	3.25
	SBA-15	174013	2.93	102.1	23.7	3.44
Bimodal by physical mixture	MCM-41 + SBA-15	280941	2.52	113.4	32.6	3.41
	SBA-15 (60 °C) + SBA-15	231892	2.38	116	30.8	3.37
Bimodal by direct synthesis	Bimodal-1	233360	2.21	111	31.3	3.21
	Bimodal-2	261126	2.17	112.4	32.9	3.15

merization catalytic activity than homopolymerization (negative comonomer effect), which, as previously mentioned, should be due to the high comonomer concentration employed in the synthesis.

Tables 2 and 3 summarize the properties of polyethylenes homo and copolymers respectively. Molecular weight of homopolyethylenes obtained with supported catalysts over unimodal porous distribution carriers increases as pore size becomes smaller, which is in accordance with results presented by F. Silveira et al.[13] Small pore diameter can limit the monomer access to the catalyst centre reducing the activity but affording a larger polymeric chain growth through a mechanism known as ''extrusion polymerization'' in which the growing polymer starts from metallocene's centre grafted inside the mesopores.[28] However, bimodal porous distribution carriers do not lead to significant differences in the molecular weight of polyethylenes obtained with them.

Melting temperatures and crystallinities also follow the same trend as molecular weight. A comparison between homopolyethylene and ethylene-1-hexene copolymers properties reveals that molecular weight is not affected by the comonomer or an increment of that value for copolymer takes place (mainly for bimodal porous distribution supports).

Catalysts with wider pores can incorporate higher 1-hexene contents perhaps due to the faster diffusion rate of the bulkier 1-hexene molecules into supports with larger pore diameters. On the other hand, the incorporation of these short branches coming from 1-hexene incorporation decreases the melting temperature and crystallinity in comparison with the homopolymer, as it was expected.

Chemical composition distributions determined by Crystaf (Figure 8) disclose a heterogeneous composition for most of the copolymers. Homopolymers display unimodal and narrow CCDs with maximum peak temperatures quite similar between them. CCDs of copolymers synthesized with the catalytic system over unimodal pore distribution materials becomes broader as the pore size increases, showing a bimodal CCD for SBA-15 material, which was previously reported.[29] The physical mixture MCM-41 + SBA-15 is less bimodal

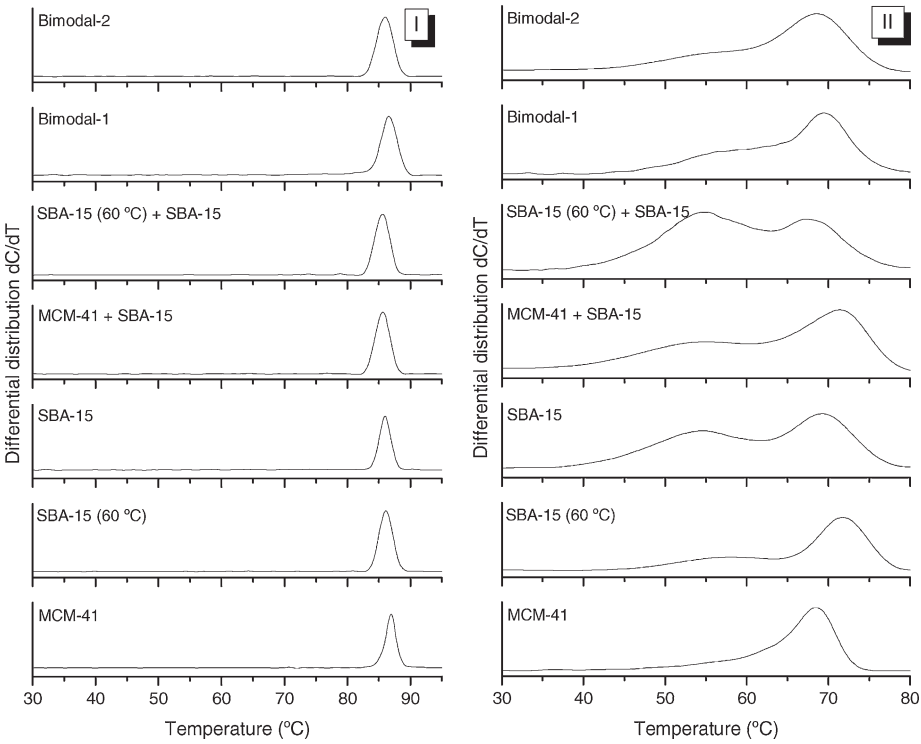

Figure 8.
Chemical composition distributions of I: ethylene homopolymers and II: ethylene-1-hexene copolymers obtained with the catalytic system MAO/$(nBuCp)_2ZrCl_2$ supported over different siliceous materials.

than SBA-15 (60 °C) + SBA-15, as individual MCM-41 lead to unimodal CCD while SBA-15 gave a copolymer with bimodal CCD. On the other hand, bimodal carriers by synthesis depicted a bimodal CCD but softer (less prominent) than physical mixtures which is supposed to be related with the higher ratio of small pore/large pore (both channel systems with similar contribution to the total pore volume) of the physical mixtures compared with the synthetic route.

Conclusion

Synthesis procedures used for preparing supports with a bimodal pore size distribution leads to materials with quite different contribution of each pore system to the total porosity whereas physical mixtures of two different supports (prepared with a mass ratio 1:1) allow to obtain similar contribution of each mesophase.

In general, catalysts with larger pores presented higher activity in ethylene polymerization despite the presence also of smaller pores like in catalysts prepared with bimodal pore size distribution supports. The same trend was observed for comonomer incorporation in the ethylene/1-hexene polymerizations.

Apart from MCM-41, catalytic behavior observed for copolymerization reactions show a negative comonomer effect for all the supports because of the high 1-hexene concentration employed. Differences between homopolymerization and copolymerization seem to be higher when the pore size increases.

Regarding to polymer properties, all the polyethylenes obtained present unimodal molecular weight distributions but a clear bimodality is noted for chemical composi-

tion distributions of ethylene/1-hexene copolymers. Higher pore size leads to broader CCD obtaining a bimodal CCD by using SBA-15 as catalytic support. Bimodal pore size distribution supports (physical mixtures and direct synthesis) lead to more prominent bimodal CCD when they have both channel systems with a more similar contribution to the total pore volume.

[1] H. Knuuttila, A. Lehtinen, A. Nummila-Pakerinen, *Adv. Polym. Sci.* **2004**, *169*, 13.
[2] WO 2006108512 (2006), Borealis Techology Oy, I. Helland, S.S. Eggen, R. van Marion.
[3] WO 2010008964-A1 (2010), Innovation Technologies LLC. H. Liu, C. R. Mure.
[4] H. Knuuttila, A. Lehtinen, H. Salminen, "*Metallocene-Based Polyolefins*", John Wiley & Sons Ltd, 2000, 365 pp.
[5] M. Ahmadi, R. Jarnjah, M. Nekoomanesh, G. H. Zohuri, H. Arabi, *Macromol. React. Eng.* **2007**, *1*, 604.
[6] L. D. Li, Q. Wang, *J. Pol. Sci.* **2004**, *42*, 6552.
[7] H. S. Cho, Y. H. Choi, W. Y. Lee, *Catal. Today* **2000**, *63*, 523.
[8] F. Silveira, M. C. Martins, F. C. Alvesa, S. B. Stedile, J. H. Pergherb, dos. Santos. Zimnoch, *Microporous Mesoporous Mater.* **2010**, *315*, 213.
[9] M. Groenewolt, M. A. S. Polrz, *Langmuir* **2004**, 7811.
[10] J.-H. Sun, Z. Shan, T. Maschmeyer, M.-O. Coppens, *Langmuir* **2003**, *19*, 8395.
[11] D. Zhao, J. Feng, Q. Huo, N. Melosh, G. H. Frederickson, B. F. Chmelka, G. D. Stucky, *Science* **1998**, *279*(5350), 548.
[12] W. Lin, Q. Cai, W. Pang, Y. Yue, B. Zou, *Microporous Mesoporous Mater.* **1999**, *33*, 187.
[13] F. Silveira, C. F. Petry, D. Pozebon, S. B. Pergher, C. Detoni, F. C. Stedile, J. H. Z. dos Santos, *Appl. Catal. A-Gen.* **2007**, *333*, 96.
[14] P. Kumkaew, S. E. Wanke, P. Praserthdam, C. Danumah, S. Kaliaguine, *J. Appl. Polym. Sci.* **2003**, *87*(7), 1161.
[15] P. Kumkaew, L. Wu, P. Praserthdam, S. E. Wanke, *Polymer* **2003**, *44*(17), 4791.
[16] T. Sano, K. Doi, H. Hagimoto, Z. Wang, T. Uozumi, K. Soga, *Chem. Commun.* **1999**, *8*, 733.
[17] T. Sano, H. Hagimoto, J. Jin, Y. Oumi, T. Uozumi, K. Soga, *Macromol. Rapid Commun.* **2000**, *21*(17), 1191.
[18] T. Sano, H. Hagimoto, S. Sumiya, Y. Naito, Y. Oumi, T. Uozumi, K. Soga, *Microporous and Mesoporous Mater.* **2001**, *44–45*, 557.
[19] A. Carrero, R. van Grieken, I. Suarez, B. Paredes, *Polym. Eng. Sci.* **2008**, *48*(3), 606.
[20] G. B. Galland, M. Seferin, R. S. Mauler, J. H. Z. dos Santos, *Polym. Int.* **1999**, *48*(8), 660.
[21] J. H. Z. dos Santos, T. Uozumi, T. Teranishi, T. Sano, K. Soga, *Polymer* **2001**, *42*(10), 4517.
[22] M. F. V. Marques, A. B. Marinha, *J. Polym. Sci., Part A: Polym. Chem.* **2004**, *42*(12), 3038.
[23] W. Wang, L. Wang, X. Dong, T. Sun, J. Wang, *J. Appl. Polym. Sci.* **2006**, *102*(2), 1574.
[24] H. W. Park, J. S. Chung, S. S. Lim, I. K. Song, *J. Mol. Catal. A: Chem.* **2007**, *264*, (1–2), 202.
[25] M. Smit, X. Zheng, R. Bruell, J. Loos, J. C. Chadwick, C. E. Koning, *J. Polym. Sci. Pol. Chem.* **2006**, *44*(9), 2883.
[26] B. A. Krentsel, Y. V. Kissin, V. I. Kleiner, L. L. Stotskaya, *Polymers and Copolymers of Higher α-olefins: Chemistry, Technology, Applications*, 1997, 374 pp.
[27] S. Bunchongturakarn, B. Jongsomjit, P. Praserthdam, *Catal. Commun.* **2008**, *9*, 789.
[28] K. Kageyama, J. I. Tamazawa, T. Aida, *Science* **1999**, *285*(5436), 2113.
[29] B. Paredes, J. B. P. Soares, R. van Grieken, A. Carrero, I. Suarez, *Macromol. Symp.* **2007**, *257*, 103.

